

## ENERGY CONSUMPTION EVALUATION OF ROTARY TILLER USING DYNAMIC MODELLING

### EVALUAREA CONSUMULUI DE ENERGIE A FREZEI AGRICOLE FOLOSIND MODELAREA DINAMICĂ

Ferenc TOLVALY-ROȘCA, Zontán FORGÓ, Judit PÁSZTOR <sup>\*)</sup>

Sapientia Hungarian University of Transylvania, Faculty of Technical and Human Sciences, Târgu Mureș/ Romania;

Tel: +40720399662; E-mail: pjudit@ms.sapientia.ro

DOI: <https://doi.org/10.35633/inmateh-68-17>

**Keywords:** rotary tiller, computer simulation, fuel consumption, Matlab Simulink

#### ABSTRACT

Tillage is the most energy-intensive agricultural operation. In the actual energy situation it is important to explore and analyze the physical laws of soil cultivation processes, which demand increased energy, at the border of technical- and agricultural sciences. In this paper, the physical phenomena that occur during soil work with a rotary tiller were studied, and the energy requirements were approximated by computer simulation using Matlab Simulink environment. The model used was a simplified solid model of an FPP-1.3 type rotary tiller, used previously in real experiments to determine fuel consumption at various working parameters. The results obtained by the dynamic simulation were compared with the real measurements.

#### REZUMAT

Prelucrarea solului este cea mai energo-intensivă operație agricolă. În actuala situație energetică, este importantă studierea și analiza legilor fizicii, care caracterizează procesele de prelucrare energo-intensivă. În acest articol s-au studiat procesele fizice caracteristice frezării solului și s-a aproximat necesarul de energie utilizând programul de simulare Matlab Simulink. Modelul folosit a fost modelul solid simplificat a frezei de sol tip FPP-1,3, utilizat în anii precedenți în experimente reale care au urmărit determinarea consumului de combustibil pentru diferiți parametri de prelucrare. Rezultatele obținute prin simularea dinamică au fost comparate cu măsurătorile reale.

#### INTRODUCTION

Tillage is an intervention in the physical condition of the soil, in such a way that the most favorable living conditions are created for the plants. During tillage, ground cultivation and seedbed preparation are carried out. Basic cultivation means turning the soil, while bed preparation means soil shredding, loosening, mixing, surface shaping and compaction below sowing depth (Marin *et al.*, 2012).

The basic aim in tillage operations is always to provide the seedbed required for plant growing, with the least possible number of passes and minimum energy consumption. In order to reduce the number of passes, tillage machines with active tillage tools are preferred (Cujbescu *et al.*, 2019; Tenu *et al.*, 2012).

It is common for the seedbed to be prepared with a rotary tiller, which mixes, but it also shreds, loosens and levels the soil. The rotary tiller's working tools are active, and during towing, they are also driven by the power take-off shaft (the PTO). For this reason, the traction power requirement of the working machine is lower; the sliding losses are also reduced, so the rotary tiller can be also used in moist soil conditions (Usaborisut *et al.*, 2020; Vlăduț *et al.*, 2018). Cultivation with this type of machine is intensive, creates dust, increases the mineralization process of soil organic matter, and reduces the formation of hardpans (Catania *et al.*, 2018; Chen *et al.*, 2022; Hassan *et al.*, 2018).

Many researches deal with the study of the active soil tillage machines. They often visualize the operation by means of mechanical / kinematic models. Ahmadi *I.*, (2017), developed a theoretical calculator to determine the torque and power requirement of the rotary tiller. Using an Excel spreadsheet, based on the given mathematical formulas, the performance requirements of some tillage tools can be effectively predicted. Thus, the performance requirements of different tillage machines can be compared. The spreadsheet calculator is also suitable for examining the effect of a selected input working parameter on outputs.

<sup>1</sup> Ferenc Tolvaly-Roșca, Assoc.prof.; Zontán Forgó, Assoc.prof.; Judit Pásztor, Lecturer

Nowadays, studying and modeling of tillage tools is an important part in the development of new agricultural machines. The precise mechanical sizing of a new tool must be carried out before field tests, with modern mathematical-mechanical computer methods.

By computer modeling, the interaction between the tool and the soil, development time and costs can be significantly decreased (Kuan, 2020; Major and Csanády, 2014; Forgó et al., 2021). Saimbhi et al., (2004), also used computer modeling methods of the working process in their minimum tillage study, and FEM methods were used for the study of soil compaction (Ungureanu et al., 2017; Ungureanu et al., 2018). With the help of special engineering software, Tolvaly-Roşca and Pásztor, (2019), studied the trajectory of the tiller, and the shape and size of the cut soil slices, respectively.

Determining the energy demand for the tilling processes is useful both for the developers and operators of machines. Energy demand is measured in laboratory and field conditions, but it is increasingly common to determine it by computer simulation. When studying the performance requirements of the rotary tiller, it is also important to explore the forces and loads occurring on the blades during operation.

## MATERIAL AND METHODS

In the present paper an FPP-1,3 type rotary tiller was studied. In previous years, experiments regarding the real fuel consumption varying the linear speed of the tractor were lead. The results were presented in (Drunek, 2009). Using Autodesk Inventor software, a simplified solid assembly model of the rotary tiller (modeling blades without wear) was built using. The image from Figure 1 was taken a few years later with visible wear signs on the blades. Using the solid subtraction method simulating software, developed and presented in (Tolvaly-Rosca and Pásztor, 2019) the cuts for a single blade rotation were simulated, then the dislocated soil volumes for the three different advancing speed (the working speed of the tractor) of the real experiments were determined.

Using the literature (Sitkei, 1976; Căproiu et al., 1982; Aluko, 2000; Amantayev et al., 2017) and some new considerations observed after the simulations, the loads and forces acting on a single blade were determined and calculated. The solid model of the rotary tiller was imported to Matlab Simulink environment with similar procedures as those presented in (Forgó et al., 2021). The calculated forces was applied on each blade of the model, and as output of the Simulink simulation, the working trajectories of the blades, and the energy consumption of the tillage process were obtained.

In a next step of the energy evaluation, the results from the simulation and the results obtained earlier upon the field experiments were compared.

The experimental and simulation results were presented and compared.

### The FPP-1.3 Type Rotary Tiller

The FPP-1.3 type rotary tiller is intended for the superficial mixing and loosening of the soil, the crushing of clods and the destruction of weeds, the crushing and incorporation of organic fertilizers into the soil of vegetable, viticulture and fruit cultures, especially in greenhouses.

The presented rotary tiller is a suspended agricultural machine; it works in aggregate with the 33 kW tractors. The machine's main organ is the horizontal rotor with blades. The cutter rotor is driven from the tractor's power take-off through a lateral transmission. There are seven flanges on the rotor on which the blades are mounted. Three blades are fixed on the marginal flanges, and six on each of the inner flanges: three are left- and three are right sided. The blades are rigid, curved in an L shape. The rotor is covered by a casing. The casing contributes to the energetic shredding of the soil; it is leveling the processed soil and also has a human protection purpose.



Fig.1 - FFP-1.30 type rotary tiller

The main technical characteristics of the FPP-1.3 type rotary tiller are presented in Table 1.

Table 1

**Main technical characteristics of the FPP-1.3 type rotary tiller**

Tractor, kW	33
Tractor's PTO speed, rot/min	540
Rotor's spindle speed, rot/min	144–225
Angular speed of the rotor, rad/s	15,07; 16,85; 21,14; 29,55
Working depth, cm	15–20
Working width, m	1,30
Diameter of the rotor, mm	510
Number of flanges	7
Number of the blades on a flange	6 (3 on the external flanges)
Total Number of the blades	36

**The Cad Model of the Rotary Tiller**

As the energy consumption measuring experiments were made with the FPP-1.3 type rotary tiller, a simplified 3D solid assembly model of the active part of the machine was built. In a first step brand new, unused rotary tiller blades were modeled using Autodesk Inventor (Fig. 2).



Fig. 2 - The real (left) and the 3D solid model (right) of a single blade

Then, using the of modeled blades (a right-handed and a left-handed), a simplified solid assembly model of the active part was built (the shaft with the blade holding discs, the bolts and the nuts) with proper material assignments to obtain a most accurate mass of the working assembly (Fig. 3).

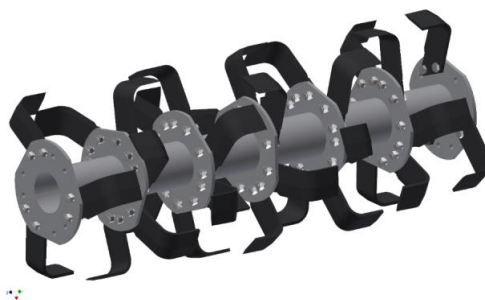
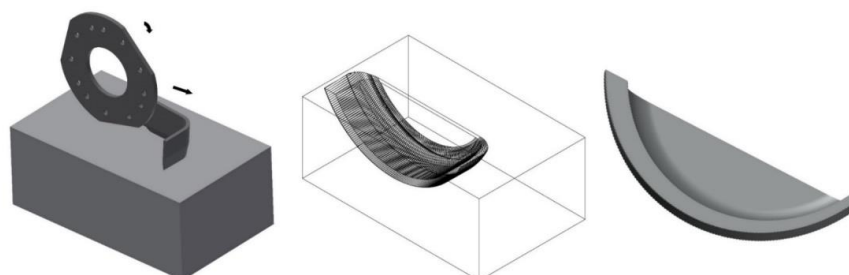


Fig. 3 - The simplified assembly model of the rotary tiller active part

During a single rotation of one blade and according on his relative movement, the solid model of rotary tiller blade was subtracted from the soil block with known volume (Fig. 4).



**Fig. 4 – Approximating the soil volume thrown by the blade**  
 Left - The cutting simulation model; Middle – The soil with the removed volume; Right – A soil slice

For the cutting simulation, the corresponding three linear advancing speeds and the spindle speed from the real experiments was used (Table 2). Where  $v_a$  is the advancing and  $v_p$  is the peripheral speed of the blades.

Reading the remained soil volume, and calculating the difference from the initial volume, an approximation of the removed soil volume was calculated and used in the further calculation.

Table 2

**Approximation of the directly dislocated soil slice volumes at different advancing speeds**

Advancing speed $v_a$	Angular speed of the rotor $\omega$	Spindle speed of the rotor	Dislocated soil volume $V$	Peripheral speed of the rotor $v_p$	$v_p/v_a$ $\lambda$
[m/s]	[rad/s]	[rpm]	[mm <sup>3</sup> ]	[m/s]	[u.l.]
0.50	15.07	146.91	1048942.6	3.843	7.67
0.57	15.07	146.91	1034835.5	3.843	6.76
0.91	15.07	146.91	966676.6	3.843	4.24

In Figure 4 it can be observed that the soil slice thickness (considered in the radial direction to the rotation axis) it is not constant for a single revolution of the blade in the soil. In the deepest point of the cut, the thickness of the soil slice has its maximum value approx. 22.5 mm (after this position the soil is already shredded and loosened, and the rotation tends to throw out the soil, there is no more compression). The thickness of the slice at the start and varies according to increase of the advancing speed, between 10.44–15 mm, and it is larger than the blade thickness (8.2 mm). Based on this observation, a compacting force must be considered, force which is neglected in the literature. This force must vary according the advancing- and rotating speed ratio ( $\lambda$ ), but also according to the angular position of the blade during the rotation process.

**Loads and Forces in the Tilling Process**

Determining the forces resulting from the tillage process and the loads on the working machines is a difficult task, since the already existing stresses in the soil can also influence the reaction of the soil on the tillage forces. According to *Rajaram (2018)*, they are also recommended to be included in the models.

To determine the exact mechanical properties of different soils types in a given moment of time can be done relatively easily with modern technical measuring devices. But to evaluate them in a general model is an extremely complex task, as many individually factors are related to strength and deformation properties, such as moisture content and soil composition (*Amantayev et al., 2017; Chen et al., 2017*).

Cultivation with tillers is a very energy-intensive process. In order to study the performance requirement, it is necessary to know the working way of the blade and the characteristics of its interaction with the soil. This mechanical work consists in two main stages:

- The working way of a rotary tiller: the blade penetrates the soil, cuts off a soil slice, accelerates it and throws it away. The thrown piece of soil hits the cover plate, where it further crumbles.
- In our study, the work performed by the rotary tiller is divided into two elementary processes: the separation process of the ground slice and the dislocation process of the soil slice (*Sitkei, 1976*).

In these two stages, according to elementary processes, four type of loads can be considered, with the following forces (Fig. 5):

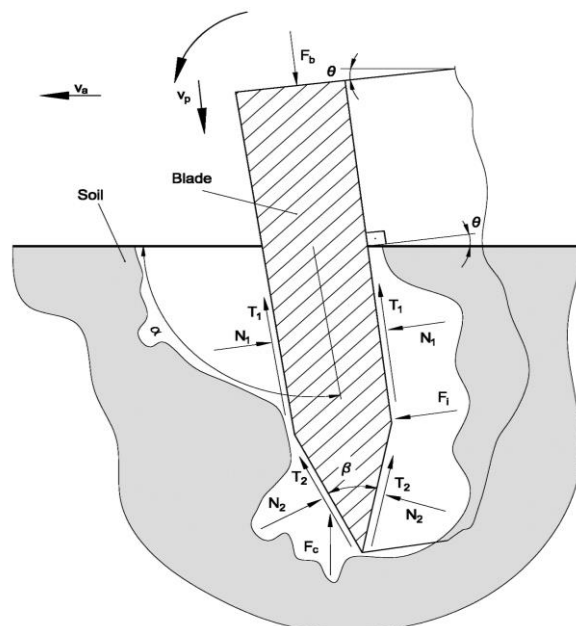


Fig. 5 – Forces acting in the working process

- the frictional forces ( $T_1$  and  $T_2$ ), acting on the sides of the blade;
- the normal forces ( $N_1$  and  $N_2$ ), acting on also on the blade sides;
- the compacting force  $F_c$ , assumed from the dislocated soil slice model;
- the inertial force  $F_i$ , given by the throwing process of the dislocated soil parts.

A fifth force, the cutting force, present most literature, noted here with  $F_b$ , is given by the frictional- and normal forces.

### The bite forces

The forces acting on the blade are shown in Figure 5. To determine the cutting force (or the bite force in the literature, noted with  $F_b$ ), blade penetration into the soil is considered as a planar movement, and the blade as a wedge with small thickness (*Aluko and Seig, 2000; Amantayev et al., 2017; Sitkei, 1976*).

Cutting the soil with the blade is considered a clean cut. The resistance of the wedge is given by the sum of the normal forces  $N$  and the frictional forces  $T$  acting on the wedge (Equations 1-4). The occasional concentrated load (stone, root) acting on the edge of the tool is not taken into account (*Sitkei, 1976*). The value of the cutting force ( $F_b$ ) is calculated with (7) considering the two active parts of the blade: the cutting force acting along the shorter wedge, the wedge perpendicular to the advancing direction of the machine, and the cutting force acting along the longer wedge, the one parallel with the advancing direction. The first one noted with  $F_{b1}$  from the moment of the contact with the soil can be considered a constant force and is calculated using (5). The second force, noted  $F_{b2}$ , depends on the angle  $\theta$ , the angle between the soil surface and the direction of the longer (the mounted) blade segment (Fig. 5), and is calculated using (6).

$$N_2 = k_{sh} \cdot A_2 \text{ [N]} \quad (1)$$

$$T_2 = \mu \cdot N_2 = \mu \cdot k_{sh} \cdot A_2 \text{ [N]} \quad (2)$$

$$N_1 = k_p \cdot A_1 \text{ [N]} \quad (3)$$

$$T_1 = \mu \cdot N_1 = \mu \cdot k_p \cdot A_1 \text{ [N]} \quad (4)$$

$$F_{b1} = 2 \cdot k_{sh} \cdot A_{21} \cdot \left( \sin \frac{\beta}{2} + \mu \cdot \cos \frac{\beta}{2} \right) + 2 \cdot \mu \cdot k_p \cdot A_{11} \text{ [N]} \quad (5)$$

$$F_{b2} = \left[ 2 \cdot k_{sh} \cdot A_{22} \cdot \left( \sin \frac{\beta}{2} + \mu \cdot \cos \frac{\beta}{2} \right) + 2 \cdot \mu \cdot k_p \cdot A_{12} \right] \sin \theta \text{ [N]} \quad (6)$$

$$F_b = F_{b1} + F_{b2} \quad (7)$$

where:  $\mu$  is the friction coefficient between the soil and the blade and it was chosen from (*Sitkei, 1976*) at a value of 0.61; and  $\beta$  is the wedge angle of the blade, measured at  $17^\circ$ .

The  $k_{sh}$  and  $k_p$  are the specific resistance to soil deformation [N/m<sup>2</sup>] on the sharpened and the parallel surfaces;  $A_1$  is the summed surface of both of the parallel sides of the blade in contact with the soil [m<sup>2</sup>], and it is composed from two  $A_{11}$  (for the shorter blade part) and two  $A_{12}$  (for the longer, mounted blade part) surfaces;  $A_2$  is the active surface formed by the two sharpened surfaces of the blade [m<sup>2</sup>], composed also from two sub surfaces two  $A_{21}$  and two  $A_{22}$ , surfaces of the shorter and respectively the longer blade parts.

The normal ( $N$ ) and frictional ( $T$ ) forces 1 and 2 indices are corresponding to above notations of the surfaces  $A_1$  and  $A_2$ .

### The inertial force

The inertial force  $F_i$  acting on the blade is given by the lift- and the throw process of the soil slice. The displaced soil's mass is approximated using the solid subtraction method to determine the volumes from Table 2, then using the Equation (8) to obtain the magnitude of the inertial force:

$$F_i = V \cdot \rho_{soil} \cdot a_s \text{ [N]} \quad (8)$$

where:  $\rho_{soil}$  is the density of the soil [kg/m<sup>3</sup>];  $V$  is the volume of the lifted and thrown soil chip [m<sup>3</sup>];  $a_s$  is the displaced soil acceleration [m/s<sup>2</sup>].

### The compacting force

The compacting force is neglected in the literature. Using solid modeling procedures, can be observed that the thickness of the cut soil slice varying alongside the blade trajectory. Due this fact, we concluded that must be acting a compression force (compacting force), which tends to compress the part of the soil in front of the blade. The exact physical phenomenon is a very complex one; it depends from the soil structure, moisture and cohesion state of the soil. This force also varies with the advancing- and rotating speed ratio ( $\lambda$ ).

To calculate the soil compaction force  $F_c$ , the Reece equation from (Cardei et al., 2019) was applied to the specific position of the blade. The compression resistance per unit width in case of the rotary tiller's blade is calculated using the Equation (9) considered for a wide blade. The maximum magnitude of the compacting force depends from the width of the blade Equation (10) and the magnitude of  $F_c$  changes according to the position of the blade Equation (11), but also according to the advancing- and rotating speed ratio ( $\lambda$ ). As the differences between the advancing speeds are smaller, we considered that the Reece's equation can be used and the effects of different  $\lambda$  values can be neglected to simplify the calculations. The  $\theta$  angle of the blade can be seen in Figure 5.

$$f_c = \gamma \cdot a^2 \cdot N_\gamma + c \cdot a \cdot N_c \left[ \frac{\text{N}}{\text{m}} \right] \quad (9)$$

$$F_{cmax} = f_c \cdot l \text{ [N]} \quad (10)$$

$$F_c = F_{cmax} \cdot \sin \theta \text{ [N]} \quad (11)$$

where:  $a$  is the width of the blade [m],  $\gamma$  is the specific gravity of the soil [ $\text{N}/\text{m}^3$ ];  $c$  is cohesion of the soil [ $\text{N}/\text{m}^2$ ],  $N_\gamma$ ,  $N_c$  are Reece type resistance factors (dimensionless);  $l$  is the length of the blade's cutting edge;  $\theta$  is the angle between the plan containing the blade's edges and the soil surface. According to the literature (Cardei et al., 2019; Sitkei, 1976):  $\gamma = 14715 \text{ N}/\text{m}^3$ ,  $c = 150 \text{ N}/\text{m}^2$ ,  $N_\gamma = 9$  and  $N_c = 5$ ; and from the measurements:  $a = 82 \text{ mm}$ ,  $l = 115 \text{ mm}$ .

The calculated  $F_c$  from Equation (11) was introduced in the Simulink model, and his variation according to the advancing- and the peripheral speed ratio  $\lambda$  was included in the computer model, as these speeds were already included in the computer model's input.

Table 3 contains the magnitude of the calculated forces, determined using Equations (1-11).

**Table 3**

**The magnitude of the forces acting on the blade**

$F_b$	$F_i$		$F_c$
[N]	[N]		[N]
$F_{b1} = 174.99$	$v_{a1} = 0.50 \text{ m/s}$	112.55	$F_{cmax} = 109.48$
$F_{b2max} = 309.20$	$v_{a2} = 0.57 \text{ m/s}$	110.84	
	$v_{a3} = 0.91 \text{ m/s}$	103.032	

## RESULTS

### Field Experiments

Fuel consumption experiments of the rotary tiller were carried out in April 2009 in the greenhouses of the Research - Development Station for Fruit Culture, Băneasa-Bucharest, and were presented in details in Drunek (2009).

Energy consumption during working with the cutter was considered the energy stored in the consumed fuel. Fuel consumption when working with the rotary tiller and the idle consumption were measured at three advancing speeds, with working depth of 15 cm and length of 15m, the width of 1.30 m, i.e. on 19.5 m<sup>2</sup>.

Fuel consumption of the work was calculated with Equation (12):

$$C_{cl} = C_{cs} - C_{cg}, \text{ [cm}^3\text{]} \quad (12)$$

where:  $C_{cl}$  is the fuel consumption of the tillage work [ $\text{cm}^3$ ];  $C_{cs}$  is the fuel consumption when working with the rotary tiller, aggregated with the U445 tractor [ $\text{cm}^3$ ]; and  $C_{cg}$  is the idle consumption: tractor running with the three speeds and the FPP-1,30 is idle, suspended over the soil [ $\text{cm}^3$ ].

The total energy obtained burning the fuel  $Q_{cl}$  can be calculated using (13):

$$Q_{cl} = C_{cl} \cdot \rho \cdot H, \text{ [J]} \quad (13)$$

where:  $\rho$  – fuel density [ $\text{kg}/\text{m}^3$ ];  $H$  - the calorific power of the fuel [ $\text{J}/\text{kg}$ ]. In the calculations, the following values were considered:  $\rho = 820 \text{ kg}/\text{m}^3$  and  $H = 41 \text{ MJ}/\text{kg}$  (at 15°C).

### The Simulink Model

The assembly model of the tiller mechanism, developed using the Autodesk Inventor modeling software, was imported in Matlab Simulink environment. To simplify the simulation method, a single flange was isolated and imported; the loads acting on one single blade were taken into consideration during the simulations. The outcome of that latter is the needed torque in order to do the tilling process with one blade.

As post-simulation work, these time series data are shifted and added accordingly the distribution of the blades on a flange. After determining the needed torque for one flange, the result is multiplied by the number of working flanges: five complete flanges with six blades and two flanges (on the extremities) with only three even distributed blades. For these two flanges the calculated torque is altered accordingly.

As depicted in Figure 6, the mechanism model is extended in order to calculate and to apply the loads raised during the tilling process. Different type of blocks may be identified inside the presented model.

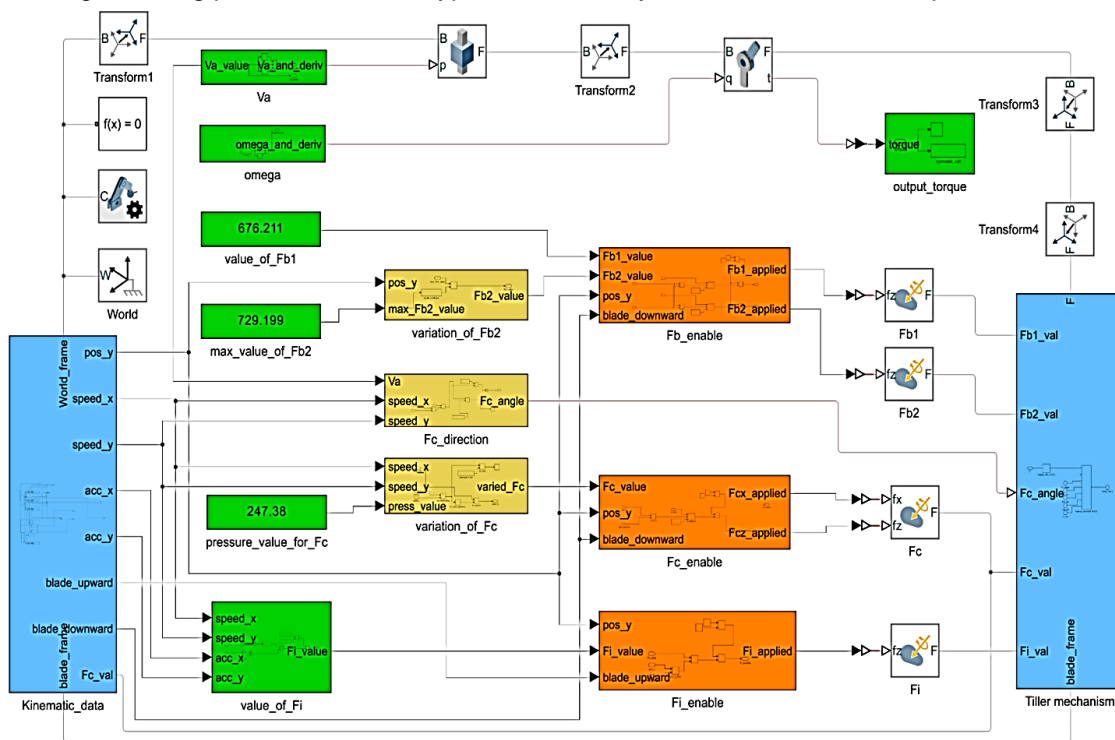


Fig. 6 – The extended model of the tilling mechanism

The blue background block (*Tiller mechanism*) contains the mechanism model and opposite of that, the other blue one (*Kinematic data*) calculates the kinematical parameters of the model regarding the world frame: the displacement, velocity and acceleration of a characteristic point (the tip) of a blade. The left side green blocks are considered the numerical input of the model: the values of the loads calculated based on Equations (5), (6), (8) and (11) are considered. Because the magnitude and direction of the loads must follow certain rules during the flange displacement and rotation (ex. the magnitude the force  $F_{b2}$  is growing from zero the value determined by Equation (6) as the blade penetrates the soil), they are altered by the yellow background blocks. The orange-colored blocks take care for the timing of the forces, they should load the mechanism at particular intervals (ex. the bite force acts only if the blade is moving downward inside the soil), and so these blocks are the enablers for that. During the simulation run, the right-side green block will save the time series torque data, which will be processed after the simulation as presented above.

The presented simulation process was applied using the advancing speed and angular speed values of the rotor from Table 2. The resulting torque's graphs (Fig. 7) are showing an even dispersion for their value during the simulations, so mean torques can be calculated.

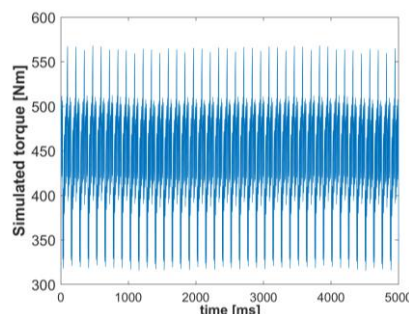


Fig. 7 – The simulated torque's graphs

Taking in account that the field experiments were made below the recommended advancing speed for tractors (0.5–0.9 m/s), the efficiency of the Diesel engine considered at 42% and transmission losses at 5%, the mechanical energy  $Q_m$  generated by the burnt fuel can be evaluated. The measured and calculated values regarding the fuel and energy consumption can be seen in Table 4.

Table 4

Fuel consumption and calculated energy values obtained in the field experiment (Drunek, 2009)

Working speed $V_a$	Fuel consumption of the work $C_{cl}$	Caloric energy $Q_{cl}$	Mechanical energy $Q_m$
[m/s]	[cm <sup>3</sup> ]	[J]	[J]
$v_{a1}=0.50$	18.58	624659.6	231124.052
$v_{a2}=0.57$	17.58	591039.6	218684.652
$v_{a3}=0.91$	16.46	553385.2	204752.524

The necessary mechanical energy for the tilling process from the computer simulation is calculated, multiplying the mean torque with the known angular displacement of the rotor. The results are presented in Table 5.

Table 5

Mechanical energy determined by simulations

Working speed $V_a$	Angular speed of the rotor $\omega$	Mechanical energy (simulation) $Q_m$	Mechanical energy (experimental) $Q_m$	Deviation	Total experimental mechanical energy	Simulated mech. energy + experimental idle energy	Deviation
[m/s]	[rad/s]	[J]	[J]	[%]	[J]	[J]	[%]
$v_{a1}=0.50$	15.07	204053.61	249863.84	-11.7	653492.112	654219.985	-0.12
$v_{a2}=0.57$		180180.56	236415.84	-17.6	635135.592	609826.456	4.7
$v_{a3}=0.91$		113602.63	221354.08	-44.5	615084.624	578549.77	7.3

Table 5 is also summarizing the energy values from the simulated mechanical work and the energy used for towing from the field experiments (idle energy). This is necessary to evaluate the predicted total (from simulation) energy compared to the results from the experiments.

The energy values obtained with the simulation, excluding the idle energy consumption, gives the mechanical work's energy requirement. Compared to the similar mechanical energy deduced from the fuel consumption in the field experiments, shows lower values, and they also depend from the advancing speed.

The deviation from the experimentally deduced values varies between -11.7% and -44.5%. As it can be seen in Figure 9, the simulated working energy (orange color), shows also a decreasing tendency compared to the experimental values (gray line).

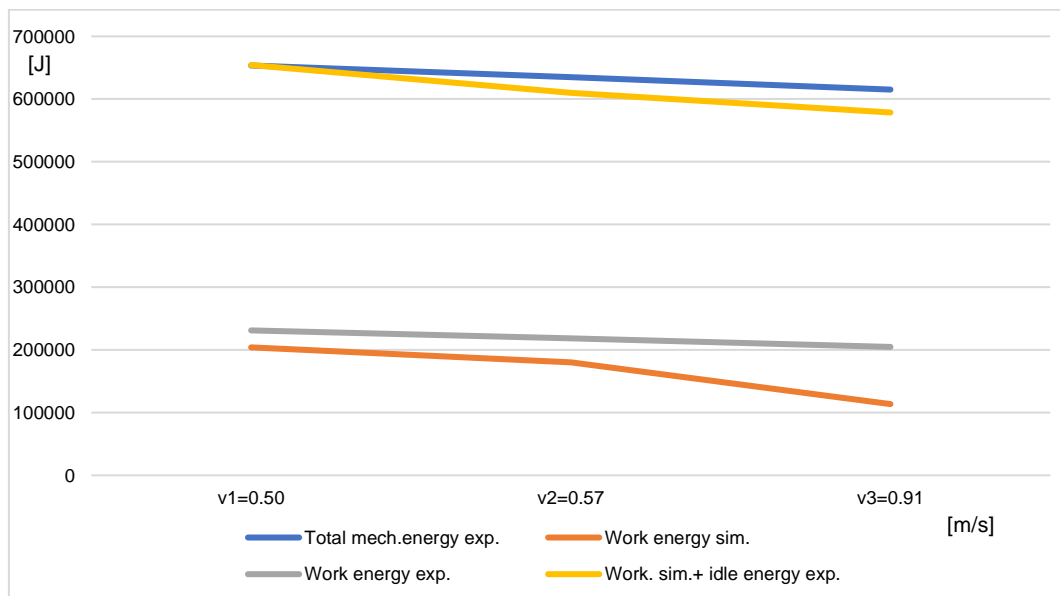


Fig. 9 – Energy consumption comparison graphs

The difference between the two energy increases with the advancing speed. The field experiments contain all the type of losses arising in a real a real working process. The minimum difference of -11.7%, consists in losses not calculated in the simulation (i.e. transmission losses at 5%, tire slipping etc.). But the increase of the difference from -11.7 % to 44.5% may be confusing at a first look.



## CONCLUSIONS

The explanation for the increasing value of the deviation between the experimental and simulated working energy, with the increase of the advancing speed, can be found in the literature: considering the rotor a traction wheel, a part of the working energy it is transformed in a pushing energy for the working unit. According to equation of this energy it varies directly proportional with the  $v_a$  working speed. It means that the real working energy deduced from the field experiments must be reduced, according to the increase of the advancing speed.

Taking in consideration this phenomenon, it is obvious that the curve of the experimental working energy (gray line) slopes down more steeply. The exact value of this transformation it was not taken in consideration at the time of the experiments, its determination requires new experiments. Regardless to these differences the developed method shows a very good approximation of the energy needs in the rotary tilling process. This can be concluded more accurately following the total energy spent for the whole working process: the blue line from Figure 9 shows the variations of the total mechanical energy deduced in the field experiments, compared to the total energy calculated from simulation and the experimental idle energy (yellow line). It varies between -0.12% and 7.3%, according to the advancing speed variation, and normally also includes the difference given by the transformation of a part of the working energy in a pushing energy of the whole unit. With this simulation values a fuel consumption can be predicted and used in field works.

The simulation method developed and applied in this paper to the spading machine in the previous work, was also applied with sufficient precision to the rotary tilling machine. Using CAD modeling methods and numerical simulations, the forces acting during soil processing by tiller were studied and analyzed.

Precise modeling of all physical phenomena that occur during agricultural work is almost impossible to achieve, due to the variety of soil types and the parameters that influence the different soil processing processes. An assessment with sufficient accuracy of fuel consumption for different parameters of the work process for different tillage processes, if it is fast as well, as in the case of the presented method, could be a particularly useful tool in modern agriculture. To predict more precisely the total energy consumption of the whole working process more field experiments need to be done, but even at the present stage of our work, a sufficiently precise prediction of the fuel consumption can be made and used in the real field works.

## REFERENCES

- [1] Ahmadi I. (2017). A torque calculator for rotary tiller using the laws of classical mechanics. *Soil and Tillage Research*, vol. 165, ISSN 0167–1987, pp.137–143, Netherlands;
- [2] Ahmadi I. (2021). Application of MS Excel to Estimate Power Needs of Tillage Tools. *Journal of Agricultural Machinery*, vol. 11, no. 1, ISSN 2423–3943, pp. 123–130, Iran;
- [3] Aluko, O.; Seig, D. (2000). An experimental investigation of the characteristics of and conditions for brittle fracture in two-dimensional soil cutting. *Soil and Tillage Research* vol. 57 issue 3, ISSN 0167–1987, pp. 143–157, Netherlands;
- [4] Amantayev, M.; Gaifullin, G.; Nukeshev, S. (2017). Modelling of the Soil-Two-Dimensional Shearing Tine Interaction. *Bulgarian Journal of Agricultural Science* 23, no. 5, ISSN 2534-983X, pp. 882–885, Bulgaria;
- [5] Cardei P., Muraru S.L., Sfiru R., Muraru V. (2019). General Structure of Tillage Draft Force. Consequences in Experimental and Applicative Researches. *INMATEH - Agricultural Engineering*, vol. 59, no.3, ISSN 2068–2239, pp. 253–262, Bucharest/Romania;
- [6] Catania P., Badalucco L., Laudicina V.A., Vallone M. (2018). Effects of tilling methods on soil penetration resistance, organic carbon and water stable aggregates in a vineyard of semiarid Mediterranean environment. *Environmental Earth Sciences*, vol. 77, no. 348, ISSN 1866–6299, pp.1–9, Germany;
- [7] Chen, K.; Cai, Z.; Hou, Z.; Qu, C. (2017). An Experimental Device for Measuring Cutting Forces of a Cutting Tool. *Advances in Engineering Research. 5<sup>th</sup> International Conference on Mechatronics, Materials, Chemistry and Computer Engineering 2017*, vol. 141, ISSN 2352–5401, pp. 1257–1260, Chongqing/China;
- [8] Căprioiu Șt., Scripnic, V., Babiciu, P., Ciubotartu., C, Roș, V. (1982). *Agricultural machinery for tillage, sowing and crop maintenance (Mașini agricole de lucrat solul, semănat și întreținere a culturilor)*, Didactic and Pedagogic Publishing House (Editura didactică și pedagogică), Bucharest/Romania;

- [9] Chen W., Ding Y., Tashi N., Zhu J., Yuan D., Yao K., Xia M., Sun L. (2022). Design and experiment of a vertical rotary tillage machine with fixed-layer fertilization function. *INMATEH - Agricultural Engineering*, vol.67, no. 2, ISSN 2068–2239, pp. 33–40, Bucharest/Romania;
- [10] Cujbescu D., Ungureanu N., Vlăduț V., Persu C., Oprescu R., Gheorghită E. (2019). Field testing of compaction characteristics for farm tractor universal 445. *INMATEH - Agricultural Engineering*, vol. 59, no. 3, ISSN 2068–2239, pp. 245–252, Bucharest/Romania;
- [11] Drunek (Pásztor) J. (2009). *Researches on the Energy Optimization of the Preparation Works of the Germination Bed in Greenhouses (Cercetări privind optimizarea energetică a lucrărilor de pregătire a patului germinativ în sere)*, Phd dissertation, Transilvania University Braşov.
- [12] Forgó Z., Tolvaly-Roşca F., Pásztor J., Kovari A. (2021). Energy Consumption Evaluation of Active Tillage Machines Using Dynamic Modelling. *Applied Sciences*, vol.11, no. 14, art. ID 6240, ISSN 2076–3417, pp. 1–17, Switzerland;
- [13] Hassan S., Nawi M. A. M., Khor C. Y., Jamalludin M. R., Wan Mohd Faizal Wan Abd Rahim, Ishak M.I., Rosli M. U., Zakaria M. S. (2018). The effect of rotary tiller blade design on soil pulverization. *AIP Conference Proceedings 2030*, 020099, issue 1, ISBN: 978-0-7354-1752-6, pp. 1–5, Vietnam;
- [14] Kuan Q., Xiaolong L., Chengmao C., Liangfei F. (2020). Relationship between soil movement and power consumption in a furrow-opening rotary blade. *INMATEH-Agricultural Engineering*, vol. 62, no. 3, ISSN 2068–2239, pp. 55–68, Bucharest/Romania;
- [15] Major, T., Csanády, V. (2014). Application of numerical analysis for the design of rotating tool. *Hungarian Agricultural Engineering*, no. 26, HU ISSN 2415–9751, pp. 16–19, Hungary;
- [16] Marin E., Pirnă I., Sorică C., Manea D., Cârdei P. (2012). Studies on structural analysis of resistance structure as a component of equipment with active working parts driven to deeply loosen the soil. *INMATEH-Agricultural Engineering*, vol.36, no. 1, ISSN 2068–2239, pp. 13–21, Bucharest/Romania;
- [17] Rajaram, G. (2018). *Mechanical Behavior of an Agricultural Soil*. Ph.D. Thesis, Iowa State University, Ames, IA, USA.
- [18] Saimbhi, V.S., Wadhwa, D.S., Grewal, P.S. (2004). Development of a Rotary Tiller Blade using Three-dimensional Computer Graphics. *Biosystems Engineering*, vol. 89, issue 1, ISSN 1537–5110, pp.47–58, United States;
- [19] Sitkei, G. (1976). *Soil Mechanics Problems of Agricultural Machines*. Franklin Book Programs, New York/ USA.
- [20] Tenu I., Carlescu P., Cojocariu P., Rosca R. (2012). *Resource management for sustainable agriculture. Impact of Agricultural Traffic and Tillage Technologies on the Properties of Soil (Chapter 10)*, ISBN 978-953-51-0808-5, London/United Kingdom;
- [21] Tolvaly-Roşca F., Pásztor J. (2019). Work Process Analysis of the Machines with Working Parts Entrained in Seedbed Preparation Works (Analiza procesului de lucru al maşinilor cu organe de lucru antrenate la lucrările de pregătire a patului germinativ). *INMATEH-Agricultural Engineering*, vol. 58, no. 2, ISSN 2068–2239, pp. 9–16, Bucharest/Romania;
- [22] Ungureanu N., Vlăduț V., Biriş S.Şt. (2017). FEM modelling of soil behaviour under compressive loads. *Materials Science and Engineering*, vol 163, art. ID 012001, pp. 1–9, doi:10.1088/1757-899X/163/1/012001;
- [23] Ungureanu N., Vlăduț V., Biriş S.Şt., Paraschiv G., Dincă M., Zăbavă B. Ş., Ştefan V., Gheorghită N. E. (2018). FEM modelling of machinery induced compaction for the sustainable use of agricultural sandy soils, *Proceedings of the 46 International Symposium on Agricultural Engineering "Actual Tasks on Agricultural Engineering"*, ISSN 1848-4425, pp. 201–211, Opatija/Croatia.
- [24] Usaborisut, P., Sukcharoenvipharat, W., Choedkiatphon, S., (2020). Tilling tests of rotary tiller and power harrow after subsoiling. *Journal of the Saudi Society of Agricultural Sciences*, vol. 19, issue 6, ISSN 1658-077X, pp. 391–400, Saudi Arabia.
- [25] Vlăduț D.I., Biriş S.Şt, Vlăduț V., Cujbescu D., Ungureanu N., Găgeanu I. (2018). Experimental researches on the working process of a seedbed preparation equipment for heavy soils, *INMATEH-Agricultural Engineering*, vol. 55, no. 2, ISSN 2068–2239, pp. 27–34, Bucharest/Romania.